Combustion Control with Pressure Gradient and Development of DFB Diode Laser Sensor

Gyung-Min CHOI
School of Mechanical Engineering, Pusan National University,
30, Jangjeon-dong, Geumjeong-gu, Busan 609-735, Republic of Korea
choigm@pusan.ac.kr

In this study, the influence of pressure gradient on flame was investigated and high temporal diode laser absorption sensor was developed as basic study for active combustion control. The effect of pressure gradient on flame shape, flammable limit and nitric oxide emission were investigated under various conditions such as equivalence ratio, velocity difference between main mixture and surrounding air. For inverse pressure gradient conditions, reaction zone became longer, wide-spread and uniform, hence slight reduction of blow off limit. Nitric oxide emission also decreased with increasing inverse pressure gradient, which was resulted from low mean flame temperature. Even though the investigation of pressure gradient effect was limited to laminar flame in present study, these results demonstrate the possibility of combustion control and low nitric oxide emission by pressure gradient. As for a sensor for combustion control, we have developed high temporal diode laser absorption sensor operating near 2.0-μm. By applying developed system to long-pass cell and a premixed laminar flat flame, its ability on measurement frequency and accuracy was evaluated. Then, the system was applied to measure the gas temperature in the spray flame of liquid-gas two phase counter flow. Diode laser absorption method succeeded in obtaining path-averaged temperature of liquid fuel combustion environment regardless of droplets of wide range diameter. The successful demonstration of time series temperature measurement in liquid-gas two phase counter flow flame gave us motivation of trying to establish effective control system in practical combustion system. Path-averaged temperature measured spray flame above liquid-gas two phase counter flow flame showed qualitative reliable results. It was found that these results demonstrated the ability of real-time feedback from combustor inside using non-intrusive measurement as well as the possibility of application to practical combustion system. However, additional investigation of diode laser absorption method is necessary to provide reliable information of the turbulent flame or spray flame.

1. Introduction

It has been considered that most of combustion oscillations or combustion instabilities are caused by the feedback interaction between natural acoustic modes of combustor and oscillations of heat release rate (Rayleigh, 1945). Since such combustion oscillations or instabilities may cause noise emission and break down of the combustor, a number of studies have been conducted to make clear the mechanism and the control strategies of combustion oscillation (Samaniego, *et al.* 1993, Broda, *et al.* 1998, Di Benedetto, *et al.* 2002, Paschereit, *et al.* 1999, Lieuwen, *et al.* 2000, Gulati, *et al* 1992, Sivasegaram, *et al* 1995, Blonbou, *et al* 2000). From the viewpoint of pollution formation, NOx have a major impact on the environment and studies related to NOx reduction by passive or active control have also been conducted (Poppe, *et al*. 1998, Delabroy, *et al*. 1998, Murugappan, *et al*. 2000).

According to Rayleigh, we may easily control combustion oscillations by simply introducing an energy source out of phase with heat release rate. However, it has been demonstrated that successful control strategies use variations of combusting condition or combustors (Gulati, *et al.* 1992, Sivasegaram, *et al.* 1995, Blonbou, *et al.* 2000). Therefore, a general combustion control scheme is necessary for an effective and robust active control of combustion. To obtain important factors for control of combustion oscillations, several experimental studies have been conducted for flame-acoustic interactions in unstable combustors using phase-locked measurements (Samaniego, *et al.* 1993, Broda, *et al.* 1998). Quantitative measurements of the flames response to acoustic perturbations have also been conducted (Poinsot, *et al*. 1986, Harper, *et al*. 2001). These measurements are heavily influenced by the combustion system. Since the combustor pressure plays important roles in the flame stabilization and nitric oxide emission of turbulent combustion field (Metghalchi, et al. 1980, Liakos, et al. 2000, Thomsen, et al. 1999), it is very informative to identify the effect of combustor pressure on the flame shape and nitric oxide emission for the development of active control schemes.

To control oscillating combustion effectively, it is necessary to investigate high temporal and sensitive sensor. To accomplish these requirements, we need an advanced in-process sensing technique that can measure the gas temperature and concentrations of major species faster and more accurate. Non-intrusive temperature and concentration sensors using lasers are attractive in many situations. Vibrational and rotational spectra of gases using laser-based sensor can provide an excellent measure of pressure,

temperature, and species concentration when the detailed dependence of the spectra on these variables are known. Near-infrared diode laser absorption sensors have been applied to in-situ measurement of gas temperature and species concentration in the combusting environment (Mihalcea, et al., 1998a, Sonnenfroh, et al., 1997) Applications of diode laser have been increased drastically owing to their robustness, compactness, reasonable cost, compatibility with optical-fiber components, and relative ease of use. The target gases were H_2O (Arroyo, et al., 1993, Allen, et al., 1996), NO(Mihalcea et, al., 1998b), NO_2 (Mihalcea et, al., 1996), CH_4(Chou, et al., 1996, Nagali, et al., 1996), CO(Daniel, et al., 1996) and CO_2(Mihalcea, et al., 1998c)

In practical combustion system, flame temperature and species concentration fluctuate with temporal and spatial. Furthermore, soot or floating particles sometimes exists in combustion-driven energy. Especially, droplets do exist for the liquid flame combustion. Because the absorption method gives us path-averaged information, beam steering may restrict extension of path-length. Rapid combustion measurements, therefore, have been demonstrated in a variety of flow-field using scanned wavelength diode laser sensor (Arroyo, et al., 1993, Arroyo, et al., 1994, Baer, et al., 1993). However, it is not cleared whether the absorption measurement using diode laser sensor is applicable to spray flame or not. In general, turbulent combustion field or spray combustion restricts wavelength sweep frequency and pass-length of diode laser beam especially because of the non-uniformity in gas temperature and species concentration. Therefore, measurement of large line strength with high temporal resolution is needed for measurements of combusting field.

The objectives of present study are to investigate the influence of pressure gradient on flame shape and nitric oxide emission and to establish the non-intrusive temperature measurement method using diode laser absorption sensor and to demonstrate its possibility of application to the liquid fuel combustion environment for active combustion control.

2. Control of flame shape by pressure gradient

2.1 Experimental methods and conditions

Figure 1 shows schematics of combustor and detail of main mixture nozzle. This combustor consists of main mixture injection section and surrounding air injection section. The surrounding air was supplied through round pipe of 50mm diameter and the inlet of combustor was diffused to 55mm × 55mm. The inner cross-section of combustion chamber was 55mm × 55mm and the outlet of combustion chamber was contracted to 50mm diameter. The total length of combustion chamber was 550mm. On front and rear side of combustion chamber, a silica glass plate of 55mm × 300mm and 5mm thickness was installed to allow optical access. The mixture nozzle has a main nozzle of 8mm diameter and eight small holes (3mm) around main hole for pilot flame.

Figure 2 shows schematic diagram of combustion measurement and control of pressure gradient. The pressure gradient of combustor was controlled by suction flow rate at combustor outlet. In present study, we defined pressure index ($P^*=P_m/P_a$), where P_m and P_a indicate the measured pressure and ambient pressure, respectively. If the suction flow rate was larger than blowing flow rate, the P* became smaller than unit and inverse pressure gradient was formed in the combustor. The digital manometer was used to measure pressure in the combustion chamber. The concentration of nitric oxides was measured by a chemiluminescence analyzer (TELEDYNE, M200AH). A water-cooled sampling probe with a 1.0mm suction hole was used to sample the burned gases at the twice times downstream of the flame length. Because there were spatial fluctuations of NOx concentration resulted from flame shape, the value on the center of the cross-section was used to obtain emission index. Mean flame temperature was measured at a half-length cross-section of flame length using a type-R thermocouple of 0.1mm wire diameter. And, the

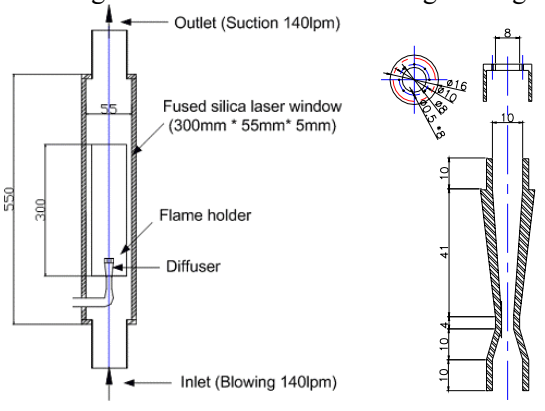

(a) Overview of combustor (b) Nozzle

Fig. 1 Detail of combustor and mixture nozzle

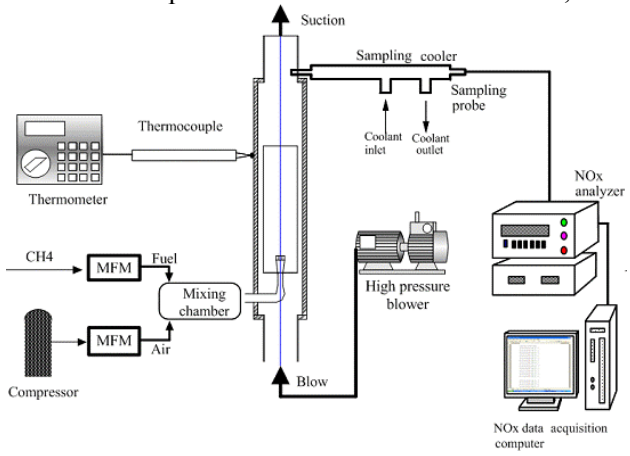

Fig. 2 Schematic of combustor and combustion measurements

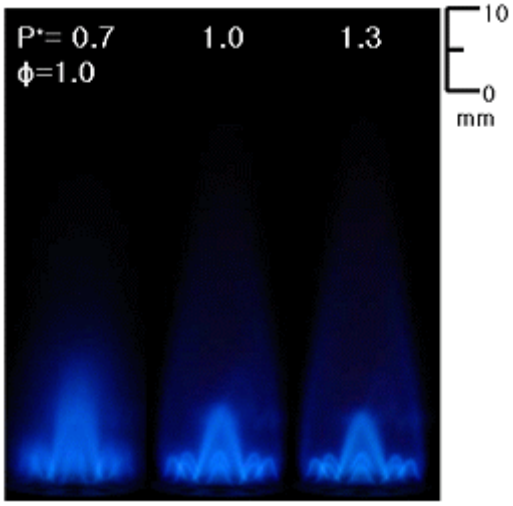

Fig. 3 Direct photography as a function of pressure gradient

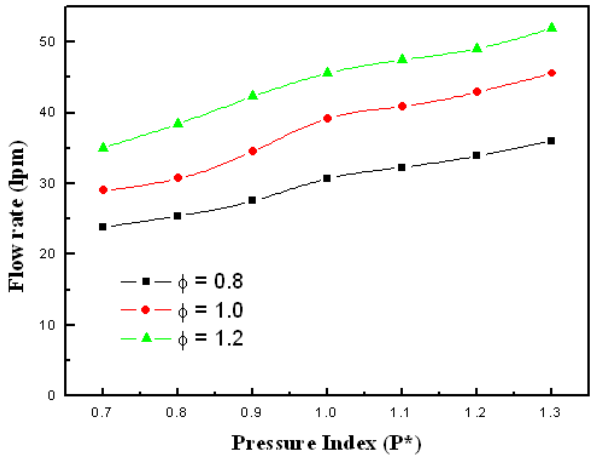

Fig. 4 Flammable limits as functions of pressure gradient and equivalence ratio

intensity of CH* band chemiluminescence was also visualized using ICCD camera (PIMAX 512) to investigate the flame structure. The jet velocity of main mixture and surrounding air are varied from 0.5 to 1.5 m/s and from 0.67 to 2.0, respectively. The equivalence ratio of main mixture is varied from 0.8 to 1.2. Methane is used as fuel of main mixture.

2.2 Combustion control by pressure gradient

Figure 3 shows direct photography as functions of pressure gradient and equivalence ratio. Mixture injected from nozzle formed primary premixed flame (inner flame) and partially unburned mixture formed secondary reacting region with emission (outer flame). Pilot flames stabilize the main premixed flame. Inner flame seems to be affected more by pressure gradient than outer flame. Stretched flame is observed at P* < 1, on the other hand, flame front can be observed obviously for P* > 1.

Figure 4 shows flammable limits as functions of equivalence ratio and pressure gradients. In Fig. 4, the points indicate the mixture flow rate where flame blows off. The stable region increases with increasing equivalence ratio and pressure index. We can observe that stable flame can be formed even in 0.7 of P*. From above results, combustion control using pressure gradient seems possible in wide range for present combustion system.

Figure 5 shows flame length as functions of pressure gradient, equivalence ratio and velocity difference between main mixture and surrounding air. We defined velocity index ($U^*=U_M/U_S$), where U_M and U_S indicate mixture jet velocity and surrounding air one. Flame length increased with decreasing pressure index for overall U* and equivalence ratio conditions. With increasing velocity index, the influence of pressure index becomes dominant. For U*=0.5 condition, the variations of flame length show almost similar tendency regardless of equivalence ratio. However, when U* becomes lager than 1.0, relatively steep slopes are observed at rich condition.

Figure 6 shows emission index of nitric oxide as functions of velocity index, equivalence ratio and pressure index. Emission index decreased with decreasing pressure index for overall velocity index and equivalence ratio conditions. The emission index values at P*=0.7 are about a quarter of that at P*=1.3. As increasing velocity index, large discrepancy with pressure index is observed in the rich condition. Above results, it is thought that we can achieve low nitric oxide combustion with suction in the outlet, and

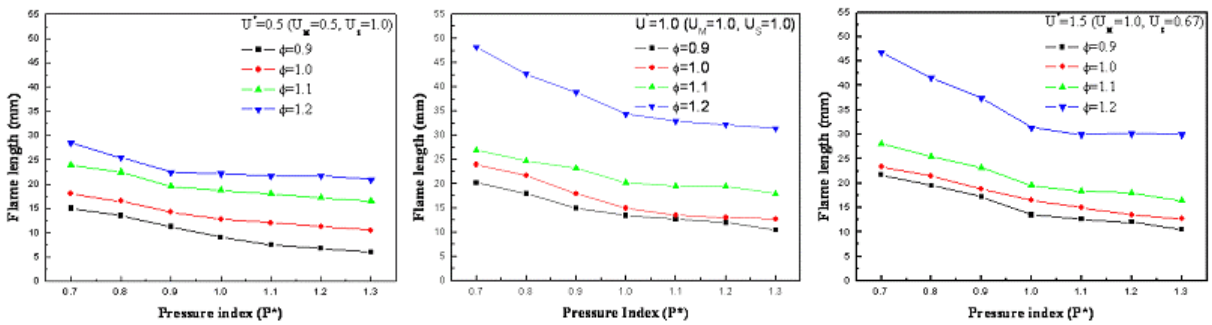

Fig. 5 Flame length as functions of pressure gradient and equivalence ratio

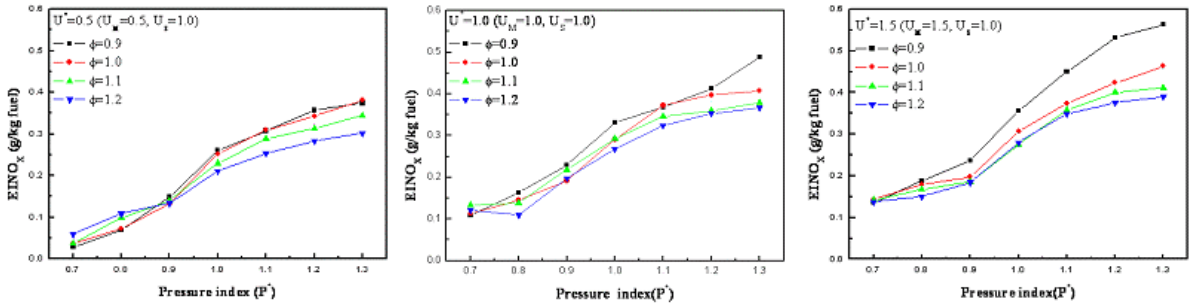

Fig. 6 Emission index of nitric oxide as functions of pressure index, velocity index and equivalence ratio

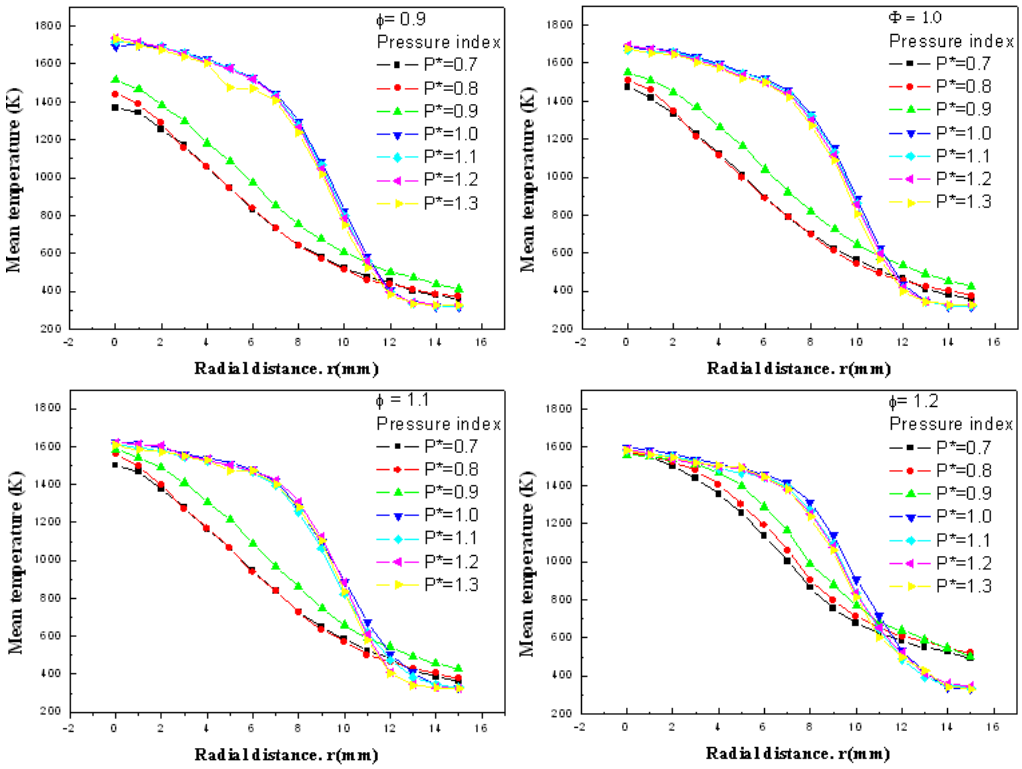

Fig. 7 Radial flame temperature distribution

this tendency is more effective at high velocity index and rich condition.

To investigate low nitric oxide emission in low pressure index conditions, we measured mean flame temperature in the half height of flame length using type-R thermocouple of 0.1mm. For all experimental conditions, mean temperature showed maximum value at the center of the combustor and it decreased with radial direction. However, quite different tendency is observed between P* ≥ 1 and P* < 1 conditions. For P* ≥ 1 conditions, mean temperature decreased monotonously from center of the combustor and then it decreased drastically at R=6-12mm region. On the other hand, for P* < 1 conditions, mean temperature decreased monotonously and it showed relatively low value compared with P* ≥ 1. From above results, we can see that the suction at outlet make the flame temperature low and uniform, hence low nitric oxide emission. The discrepancy between P* ≥ 1 and P* < 1 becomes smaller with increasing equivalence ratio.

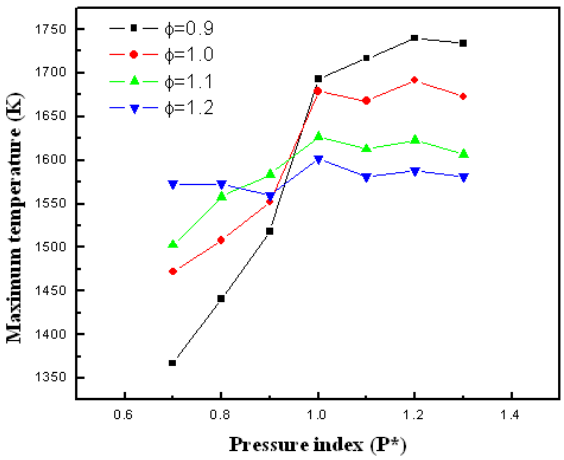

Fig. 8 Maximum flame temperature as functions of pressure index and equivalence ratio

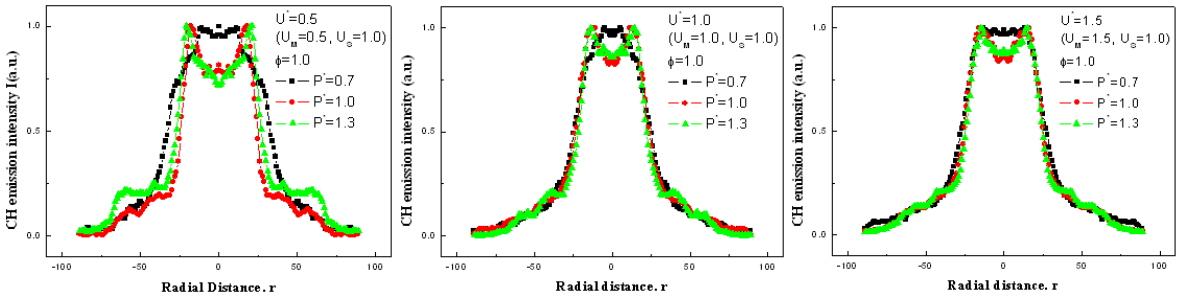

Fig. 9 CH* band chemiluminescence intensity in the radial direction

Figure 8 shows the maximum flame temperature as pressure index and equivalence ratio. The discrepancy between P* ≥ 1 and P* < 1 is obvious for lean conditions, while it becomes smaller with increasing equivalence ratio. Especially, maximum temperature changed drastically between P* =0.9 and 1.0 for lean conditions, which indicates quite small suction is effective for control of flame shape. Above results, the suction for flame shape control is more effective for under stoichiometric condition.

To investigate the change of flame shape with pressure index, we measured CH* band chemiluminescence intensity using ICCD camera shown in Fig. 9. Because measured images included line-of-sight information, Abel transformation was used. Bimodal distributions of chemiluminescence intensity are observed near center of combustor for P* ≥ 1 conditions. On the other hand, low pressure index condition show flat profile at the center of combustor. This tendency is obvious for low velocity index condition. Low nitric oxide emission at low pressure index conditions are ascribed to spread and uniform shape flames and these flames can be achieved by suction at outlet. In present study, although influence of pressure gradient has been investigated for almost laminar flames, the possibility of combustion control has been demonstrated. However, additional study should be followed to apply this technology on turbulent oscillating flames.

3. Development of DFB Diode Laser Sensor

3.1 Measuring principle of diode laser absorption sensor and its system

The measurement technique is based on the absorption of monochromatic near-IR laser radiation. The transmission of a probe beam of light through absorbing medium follows the Beer-Lambert relation as follows

$$T = \left(\frac{I}{I_0}\right)_\nu = exp(-k_\nu L) = exp\left(-P \sum_{j=1}^{K} X_j \sum_{i=1}^{N_j} S_{i,j}(T)\Phi_{\nu,i,j} L\right) \quad (1)$$

where, L is path-length in the medium, I_0 is the incident intensity of probe beam, I is intensity after propagation through a length L of the absorbing medium, and k_ν is spectral absorption coefficient at frequency ν. The spectral absorption coefficient (cm^{-1}) comprising N_j overlapping transitions in a multi-component environment of K species can be expressed as right hand term. P(atm) indicates the total pressure of the absorbing species, X_j is the mole fraction of j species, $S_{i,j}(T)(cm^{-2}/atm)$ is the line strength transition i and species j, and $\Phi_{\nu,i,j}$ (cm) is the respective line shape function of transition i at frequency ν. Its spectral integral over frequency is unity. The strategy for measuring the temperature of the gas is based on the intensity ratio of two-absorption line. The partial pressure of gas can be obtained from eqn.(1) if the temperature, line strength, and path-length are given.

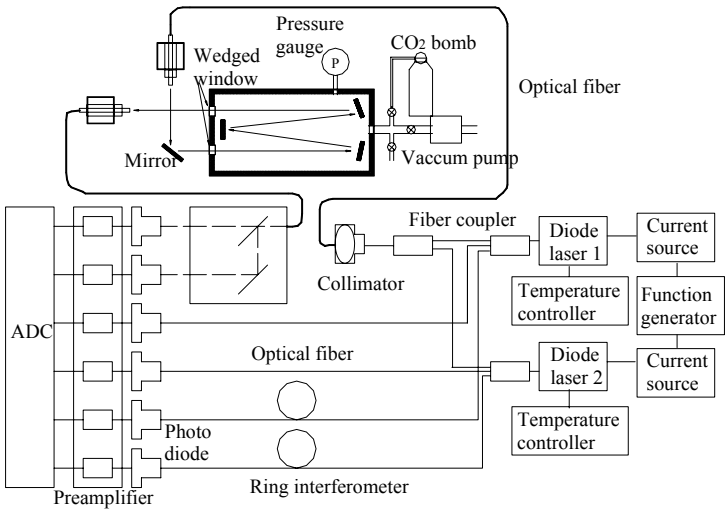

Fig. 10 Diagram of absorption coefficient measurement system

Line strengths and positions for absorption species at each temperature have been taken from HITEMP (high-temperature version of HITRAN) and HITRAN98.

This line-of-sight method may represent a significant problem and require complex reconstruction algorithms for measurement of unsteady flows such as liquid-gas two phase reacting flow. However, a reasonable estimate of the average value of gas mole fraction or temperature in the liquid fuel flames would provide useful information in present stage.

Table 1 Selected vibrotational overtones

Species	Transition Frequency (cm^{-1})	Line Strength (Temperature K) (cm^{-2}/atm)	Transition
H_2O	4878.193	1.08E-3 (1200)	(021)-(010)
H_2O	5008.101	4.91E-4 (1200)	(011)-(000)
CO_2 (R34)	4878.293	3.05E-3 (296)	(20013-00001)

Figure 10 shows the experimental setup including multi-pass cell and diode laser sensor system. The diode laser system consisted of two DFB lasers (5mW) operating near 4878cm^{-1} and 5008cm^{-1}, respectively. The wavelength of DFB lasers were scanned over selected H_2O and CO_2 transitions shown in Table 1. The repetition rate was between 0.5 and 15kHz. The output of each laser was split into three fibers, the first one for the direct absorption measurement, the second for a reference signal and the last for a fiber ring interferometer (FSR = 1.014GHz).

The beams for the direct absorption measurement, combined into a multiplexed optical fiber, were reflected many times by mirrors in the multi-pass cell to make high absorption pass/volume ratio. Thus, the pass length for the multi-pass cell was 250cm. At the exit of a receiving optical fiber, the collected beams were split into two by a dichroic mirror, and then the absorbed beam of each wavelength was detected at the photo diode. Figure 11 shows the experimental set-up including burners, a diode laser sensor system and a thermocouple. In the present work, two kinds of burner system were used.

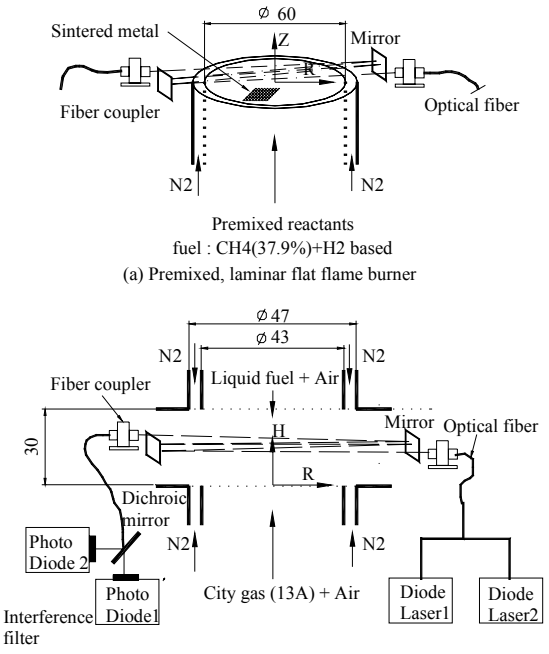

Fig. 11 Experimental schematic of in-situ combustion measurements

First, we measured species temperature and at the post-flame region on a premixed flat-flame with 6-cm diameter as shown in Fig. 11(a). Mixture of CH_4 (37.9%)+H_2 (62.1%) and air was supplied into the burner. The equivalence ratio was changed between 0.52 and 1.11. Post-flame temperature was also measured at the center of the burner port using a type-R thermocouple of 0.1mm wire diameter.

Second, we measured gas temperature in the liquid-gas two phase counter flow flame as shown in Fig. 11(b). From the upper port, n-decane ($C_{10}H_{22}$) with air is supplied, and from the lower port, city gas and air premixed mixtures are supplied. To stabilize the liquid gas two phase flame, liquid fuel is injected into the stable city gas and air-premixed counter flow flame. Liquid fuel is supplied by free fall from droplet chamber. We supplied relatively large droplet to the gaseous flame region in order to observe the interaction between droplets and gaseous flame in the wide droplet diameter range. The premixed liquid-air and city gas-air flows are supplied from the inner tube (43mm diameter). On the other hand, nitrogen is supplied from outer tube (47mm diameter) to protect mixing with surrounding air. This nitrogen jet also protects flame attachment in the burner rim. In present work, we set the distance between burners ports to 30mm(40/s strain rate). Counter flows flame without liquid fuel is formed at H=12mm, and the flame shape is almost 2-dimensional flat flame. Refraction surface is observed at H=18mm, which is estimated as the stagnation plane between the exhaust gas at high temperature and the air injected at the normal temperature from upper port. It is estimated that the exhaust gas from the premixed flat flame is accelerated by thermal expansion through combustion. The probe beams for the direct absorption measurements were reflected 5 times by mirrors to make high absorption path/volume ratio. Because the exhaust gas exists between flame front and stagnation plane, absorption coefficient measurement is carried out at H=15mm and 17.5mm.

3.2 Accuracy of sensor and combustion measurements in laminar flat flame

The performance test of this diode laser sensor system was evaluated for wide sweep frequency range. Because the main target of present work is in-situ combustion measurement for fluctuating flame with time, high temporal absorption measurements is necessary. The temporal resolution of developed sensor system was shown in Fig. 12. Selected CO_2 band (R34) has a central frequency at 4878.293cm^{-1} as shown in Table 1. Each point indicates the averaged 100 periods at each sweep frequency. The measured absorption areas were almost constant for various sweep frequencies from 0.5kHz to 10kHz. As the characteristic frequency of turbulent flame is generally thought to be below 1kHz, we can know that this diode laser sensor system has sufficient temporal resolution for in-situ combustion measurements.

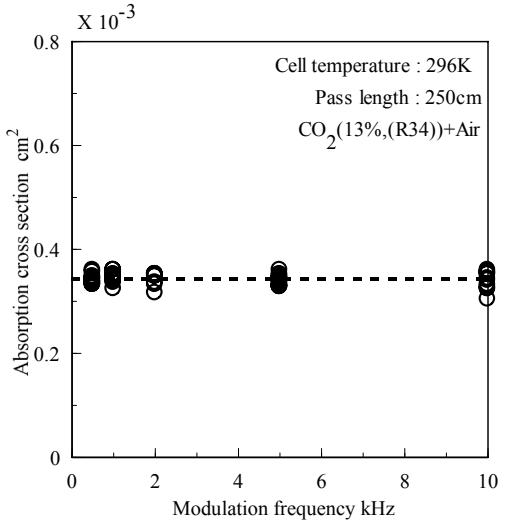

Fig. 12 Absorbance variation as a function of sweep frequency

As mentioned above, we applied this diode laser absorption sensors, of which high sensitivity as well as the performance near 2.0-μm was confirmed, to the temperature and species concentration measurement on the combusting field. For high temperature measurements, since it is not easy to measure temperature accurately, low temperature sensitivity of the line strength is desirable.

In addition, none or little spectral interference from the neighboring combustion gases is also needed. For example, H_2O has relatively large line strength than CO_2 at high temperature region. Considering these points, we selected 2 H_2O vibrotational overtones for measuring temperature and vapor concentration as shown in Table 1.

Figure 13 shows measured gas temperatures in the post-flame region of laminar flat-flame by the thermocouple and diode laser sensors as a function of equivalence ratio. The measured temperatures were nearly independent of stoichiometry due to the heat loss to the burner port. The uncertainty of the thermocouple primarily depends on radiation loss, which was estimated about 2-3%. The average difference between temperatures measured by the diode laser sensors and by the thermocouple was estimated 0.6%. Nevertheless, we observe relatively large discrepancy in rich flames. This trend may be resulted from non-uniformity of temperature in the boundary layers. If we consider the maximum discrepancy is 4.8% at ϕ=0.96, temperature measurement using diode laser sensor is acceptable.

Figure 14 shows the distribution of H_2O mole fraction as a function of equivalence ratio. The solid line is calculated values assuming chemical equilibrium for the measured temperature. The data were compensated for the possible error in H_2O mole fraction considering the non-uniformity of temperature in the boundary layer. The data are consistent within 3.4% of the equilibrium predictions for all experimental conditions. The uncertainty of species concentration depends on the magnitude of error in temperature measurement as well as the uncertainty of the line strength because the species mole fraction is determined using measured temperature and line strength. Provided that the uncertainty of temperature measurement is 4.8% at 1221K, the uncertainty of estimated H_2O mole fraction is 6.2±0.1 %.

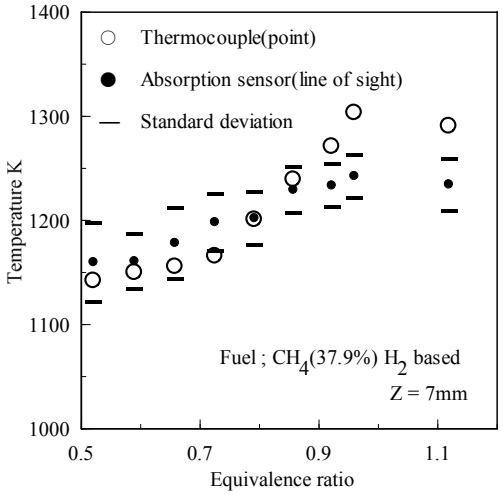

Fig. 13 Comparison of measured temperatures by diode laser absorption method with values by type-R thermocouple probe

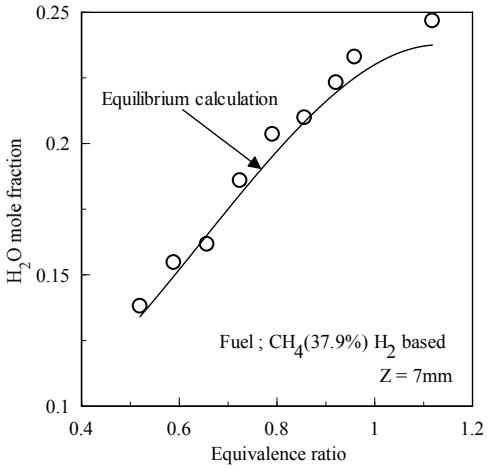

Fig. 14 Comparison of measured mole fractions of H_2O with calculated equilibrium values

3.3 Combustion measurements in liquid-gas two phase counter flame

Figure 15 shows the direct photography of liquid-gas two phase counter flame, of which shutter exposure time is 1/15 second. Measuring cross section and experimental condition are also indicated in the photography. The gaseous flame shape is distorted due to intrusion of the fuel droplets and penetration of large droplets into the reaction zone. Luminous flames are observed near stagnation plane due to liquid fuel combustion.

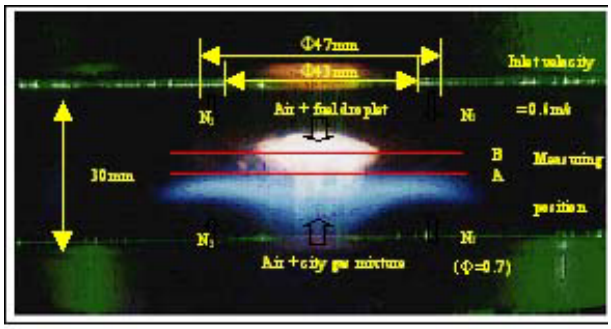

Fig. 15 Direct photography of liquid-gas two phase counter flow flame

Combustion of single droplet and droplet groups occur in high temperature region above gaseous flame in diffusion flame mode. Pre-vaporization of droplets occurs in approaching spray flow in the high temperature region. This pre-vaporization sustains the diffusion flame though 0.5 of the supplied equivalence ratio of $C_{10}H_{22}$-air mixture. The vaporization of droplets in the high temperature region works as the source of fuel vapor for burning in diffusion flame mode. No combustion reaction occurs inside the large droplet group, and burning in diffusion flame mode occurs at only the periphery. Droplet size was measured by PDA system. It was found that the droplets distributed in the wide range, and its averaged diameter was about 154μm regardless of the difference of measuring region. Figure 16 shows the single sweep of H_2O obtained from liquid-gas 2-phase counter flow flame and residuals between the direct absorption data and fitted Voigt profile. Measurement plane is at H=15mm(A), and the H_2O transition was (021)-(010) transition at 4878.193 cm^{-1}. Even though these droplets exist in the measuring region, diode laser absorption probe beam was detected at receiving optical equipment without large beam steering.

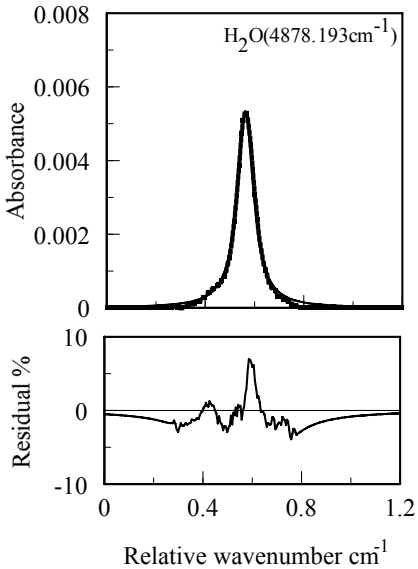

Fig. 16 Absorbance coefficients and residual distribution in the spray flame

Because the probe beam diameter was about 1mm in present work, it was possible to measure the absorption coefficient of spray flame region where droplets, of which mean diameter is 154μm, are floating in the reacting flow. However, relatively large discrepancy was observed at center frequency of single sweep between direct absorption data and fitted Voigt profile. This discrepancy is ascribed to beam steering due to droplets in the laser beam path. We used fitted Voigt profile for obtaining absorption coefficient integral in the measurement of temperature.

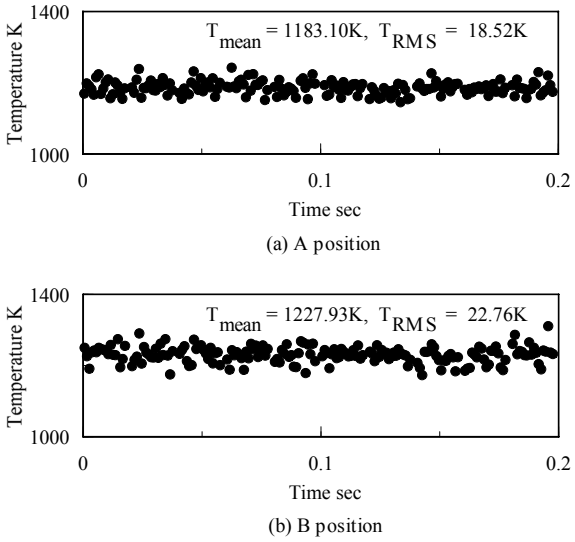

Fig. 17 Time-series temperature measured by diode laser sensors in the spray flame region of liquid-gas two phase counter flame region

Figure 17 shows the time series temperature measured by diode laser sensors in liquid-gas two phase counter flow flame. At measuring position (A), the measured mean temperature and its RMS value were 1183.10K and 18.52K, respectively. On the other hand, at the measuring position (B), mean temperature and its RMS value were 1227.93K and 22.76K, respectively. The measured mean temperature as well as its RMS value at the B position was higher than those at A region. Higher mean temperature at B region is ascribed to thicker spray flame zone as shown in direct photography of Fig. 15. As the droplet group seems to burn in the diffusion flame mode, the temperature of liquid-gas 2-phase flame is not so higher than gaseous flame. We can confirm that the temperature measurement using diode laser absorption sensor is possible

even in liquid fuel flame environment although it needs additional improvement for quantitative measurement. We did not always succeed in absorption coefficient measurement in the liquid-gas 2-phase counter flow flame. There were failure cases in obtaining absorption coefficients. These failures were ascribed to the large refraction of diode laser probe beam in the spray group combustion region above gases premixed flame. Additional investigation of diode laser absorption method is necessary to provide reliable information of the turbulent flame or spray flame.

4. Summary

In this study, the influence of pressure gradient on flame shape was investigated for various conditions such as equivalence ratio, velocity difference between main mixture and surrounding air. The flame shape, flammable limit and nitric oxide emission were measured. As increasing suction at combustor outlet, reaction zone became longer, wide-spread and uniform, hence slight reduction of blow off limit. Nitric oxide emission decreased with suction at combustor outlet, which was resulted from low mean flame temperature. These results demonstrate that flame shape and nitric oxide emission are controllable by pressure gradient. These wide-spread and uniform flame is also observed by chemiluminescence intensity. Additional study is needed for active control of turbulent oscillating flame.

We have also developed high temporal diode laser absorption sensor operating near 2.0-μm. By applying developed system to long-pass cell and a premixed laminar flat flame, its ability on measurement frequency and accuracy was evaluated. Then, the system was applied to measure the gas temperature in the post flame of gaseous counter flow flame and in the spray flame of liquid-gas two phase counter flow flame. Diode laser absorption method succeeded in obtaining path-averaged temperature of liquid fuel combustion environment regardless of droplets of wide range diameter. The successful demonstration of time series temperature measurement in liquid-gas two phase counter flow flame gave us motivation of trying to establish effective control system in practical combustion system. Path-averaged temperature measured spray flame above liquid-gas two phase counter flow flame showed qualitative reliable results. It was found that these results demonstrated the ability of real-time feedback from combustor inside using non-intrusive measurement as well as the possibility of application to practical combustion system. However, additional investigation of diode laser absorption method is necessary to provide reliable information of the turbulent flame or spray flame.

References

Allen, M. G., Kessler, W. J., (1996), AIAA J., 34:3:483-488.

Arroyo, M. P., Birbeck, T. P., Baer, D. S., Hanson , R. K., (1994), Optics letters, 19:14:1091-1093.

Arroyo, M. P., Hanson, R. K., (1993), Appl. Opt., 32:30:6104-6116.

Baer, D. S., Chang, H. A., Hanson, R. K., (1993), J. Quantitative Spectroscopy and Radiative Transfer, 50:6:621-633.

Bell, J. B., Day, M. S. and Grcar, J. F., (2002), *Proc. Combust. Inst.*, 29: 1987-1993.

Blonbou, R., Laverdant, A., Zaleski, S., and Kuentzmann, P., (2000), *Proc. Combust. Inst*., 28:747-755.

Bockle, S., Kazenwadel, J., Kunzelmann, T., Shin D.-I., Schulz, C. and Wolfrum, J., (2000), *Proc. Combust. Inst.*, 28: 279-286.

Broda, J. C, Seo, S., Santoro, R. J., Shirhattikar, G., and Yang, V., (1998), *Proc. Combust. Inst*., 27:1849-1856.

Chen, J., Echekki, T. and Kollomann, W., (1999), *Combust. Flame*, 116: 15-48.

Chou, S. I., Nagali, V., Baer, D. S., Hanson, R. K., (1996), AIAA Paper #96-0746.

Daniel, R. G., Mcnesby, K. L., Miziolek, A. W., (1996), Appl. Opt., 35:4018-4025.

Delabroy, O., Haile, E., Lacas, F., Candel, S., Pollard, A., Sobiesiak, A., Becker, H. A., (1998), *Exp. Thermal Fluid Sci.*, 16:64-75.

Di Benedetto, A., Marra, F. S., and Russo, G., (2002), *Sci. and Tech*., 174(10):1-18.

Garland, N. L., and Crosley, D. R., (1985), *Appl. Optics*, 24: 4229-4237.

Gulati, A., and Mani, R., (1992), *J. Prop. Power* 8(5):1109-1115.

Harper, J., Johnson, C. J., Neumeier, Y., Lieuwen, T., and Zinn, B. T., *AIAA Paper* #2001-0486.

Hong, B-S., Ray, A., and Yang, V., (2002), *Combust. Flame*, 128:242-258.

Jenkins, K. W. and Cant, R. S., (2002), *Proc. Combust. Inst*., 29: 2023-2029.

Lee, J. G., Kim, K., and Santavicca, D., (2000), *Proc. Combust. Inst.*, 28:739-746.

Liakos, H. H, Founti, M. A, Markatos, N. C., (2000), Applied Thermal Engineering, 20:925-940.

Lieuwen, T., and Zinn, B. T., (2000), *AIAA paper*, #2000-0707.

Metghalchi, M., Keck, J. C., (1980), Combust. And Flame, 38:143-154.

Mihalcea, R. M., Baer, D. S., Hanson, R. K., (1996), Appl. Opt. 36:4059-4064.

Mihalcea, R. M., Baer, D. S., Hanson, R. K., (1998a), AIAA 98-0237.

Mihalcea, R. M., Baer, D. S., Hanson, R. K., (1998b), Meas. Sci. Technol., 9:327-338.

Mihalcea, R. M., Baer, D. S., Hanson, R. K., (1998c), Proc. Combust. Inst., 27:95-101.

Murugappan, S., Gutmark, E. J., Acharya, S., and Kristic, M., (2000), *Proc. Combust. Inst*., 28:731-737.
Nagali, V., Chou, S. I., Baer, D. S., Hanson, R. K., Segall, J., (1996), Appl. Opt., 35:21:4026-4032.
Paschereit, C. O., Gutmark, E., and Weisenstain, W., (1999), *Physics of Fluids*, 11(9):2667-2678.
Peters, N., (1999), *J. Fluid Mech.*, 384: 107-132.
Poinsot, T., Le Chatelier, C., Candel, S. M., and Esposito, E., (1986), *J. Sound Vibr*., 107(2):265-278.
Poppe, C., Sivaegaram, S., and Whitelaw, J. H., (1998), *Combust. Flame*, 113:13-26.
Rayleigh, L. *Theory of Sound*, Dover, New York, 1945.
Samaniego, J. M., Yip, B., Poinsot, T., and Candel, S., (1993), *Combust. Flame*, 94:363-380.
Sivasegaram, S., Tsai, R. F., and Whitelaw, J. H., (1995), *Combust. Sci. Technol*. 10(5):67-83.
Sreedhara, S. and Lakshmisha, K. N., (2002), *Proc. Combust. Inst*.. 29: 2051-2059.
Sonnenfroh, D. M., Allen, M. G., (1997), *Appl. Opt*., 36:30:7970-7977.
Thomsen, D. D., Kuligowski, F. F., Laurendeau, N. M., (1999), 119:307-318.